A Novel Nondevelopmental Role of the SAX-7/L1CAM Cell Adhesion Molecule in Synaptic Regulation in *Caenorhabditis elegans*

Karla Opperman,*,[1,2] Melinda Moseley-Alldredge,*,†,[1] John Yochem,*,[3] Leslie Bell,* Tony Kanayinkal,* and Lihsia Chen*,†,[4]

*Department of Genetics, Cell Biology, and Development and †Developmental Biology Center, University of Minnesota, Minneapolis, Minnesota 55455

ORCID ID: 0000-0003-2386-7734 (K.O.)

ABSTRACT The L1CAM family of cell adhesion molecules is a conserved set of single-pass transmembrane proteins that play diverse roles required for proper nervous system development and function. Mutations in L1CAMs can cause the neurological L1 syndrome and are associated with autism and neuropsychiatric disorders. L1CAM expression in the mature nervous system suggests additional functions besides the well-characterized developmental roles. In this study, we demonstrate that the gene encoding the *Caenorhabditis elegans* L1CAM, *sax-7*, genetically interacts with *gtl-2*, as well as with *unc-13* and *rab-3*, genes that function in neurotransmission. These *sax-7* genetic interactions result in synthetic phenotypes that are consistent with abnormal synaptic function. Using an inducible *sax-7* expression system and pharmacological reagents that interfere with cholinergic transmission, we uncovered a previously uncharacterized nondevelopmental role for *sax-7* that impinges on synaptic function.

KEYWORDS *C. elegans*; *sax-7* L1CAM; GTL-2 TRPM channel; modifier gene; synaptic function

L1CAMS are cell adhesion molecules conserved in *Caenorhabditis elegans*, *Drosophila melanogaster*, and vertebrates that are important for nervous system development and function. L1CAMs share a basic body plan of six immunoglobulin-like domains and five fibronectin type III repeats in the extracellular domain, a single transmembrane domain, and a highly conserved cytoplasmic tail. These domains promote both homophilic and heterophilic interactions with diverse molecules to promote cell adhesion and regulation of signal transduction in processes that include axon guidance, myelination, fasciculation, and maintenance of neural architecture, as well as synapse formation and maintenance (Chen and Zhou 2010; Sakurai 2012).

The importance of L1CAM function in nervous system development and function is evident by the diverse neurological symptoms resulting from mutations in the human L1CAM gene family that consists of L1, NrCAM, neurofascin, and CHL1. For example, mutations in NrCAM and CHL1 are associated with autism, addiction, and schizophrenia. In addition, mutations in the X-linked L1 gene result in the L1 syndrome, the symptoms of which include **c**orpus callosum hypoplasia, mental **r**etardation, **a**dducted thumbs, **s**pastic paraplegia, and **h**ydrocephalus (CRASH) (Chen and Zhou 2010; Sakurai 2012). While the severity of these symptoms is dependent on the particular lesion in L1, it is interesting that expressivity of CRASH symptoms can vary among intrafamilial patients (Jouet *et al.* 1995; Schrander-Stumpel *et al.* 1995; Fransen *et al.* 1998). For example, a male L1 patient may exhibit severe hydrocephalus while his male sibling carrying the same allele may not present with hydrocephalus. This variable phenotypic heterogeneity suggests L1 may genetically interact with other genes for disease modification. Supporting this hypothesis is the variable association of Hirschsprung's

doi: 10.1534/genetics.114.169581
Manuscript received August 8, 2014; accepted for publication December 2, 2014; published Early Online December 8, 2014.
Supporting information is available online at http://www.genetics.org/lookup/suppl/doi:10.1534/genetics.114.169581/-/DC1.
[1]These authors contributed equally to this work.
[2]Present address: Department of Neuroscience, The Scripps Research Institute, Jupiter, FL 33458.
[3]Present address: Department of Molecular Biology, University of Wyoming, Laramie, WY 82071.
[4]Corresponding author: Department of Genetics, Cell Biology, and Development, University of Minnesota, 6-160 Jackson Hall, 321 Church St., SE, Minneapolis, MN 55455. E-mail: chenx260@umn.edu

disease (HSCR) in L1 patients with hydrocephalus (Okamoto *et al.* 1997; Parisi *et al.* 2002; Jackson *et al.* 2009; Fernandez *et al.* 2012; Takenouchi *et al.* 2012). HSCR is a complex, multigenic intestinal aganglionosis disorder where ganglion cell precursors fail to migrate to the distal gut, resulting in congenital constipation. Indeed, murine studies revealed L1 as a modifier gene in intestinal aganglionosis that is consistent with HSCR (Wallace *et al.* 2010, 2011). Additional studies on L1 as a modifier uncovered a novel role for L1 in promoting the migration and differentiation of ganglion cell precursors in the distal gut (Anderson *et al.* 2006; Turner *et al.* 2009), thus illustrating the power of modifier gene studies in identifying gene functions and cellular mechanisms.

In addition to embryonic expression, L1CAMs are also expressed in adults (Liljelund *et al.* 1994; Wang *et al.* 1998; Backer *et al.* 2002; Nikonenko *et al.* 2006), suggestive of potential L1CAM functions in mature animals that may be masked by their developmental requirement. The impairment of these potential roles may also account for some of the CRASH symptoms in the L1 disorder and possibly the autism and neuropsychiatric disorders that are strongly associated with L1CAMs. This study takes advantage of the ease in performing genetic modifier analyses in *C. elegans* to dissect the functions of the *C. elegans* L1CAM, SAX-7, which in addition to controlling dendritic branching morphogenesis, also maintains the position of neurons and their axons to preserve nervous system architecture (Zallen *et al.* 1999; Sasakura *et al.* 2005; Wang *et al.* 2005; Dong *et al.* 2013; Salzberg *et al.* 2013). Here, we provide evidence demonstrating that *sax-7* acts as a modifier of synaptic regulation, uncovering a novel nondevelopmental neuronal role for *sax-7*.

Materials and Methods

Strains

C. elegans strains, provided by the Caenorhaditis Genetics Center, were grown on nematode growth medium (NGM) plates at 21°; N2 Bristol served as the wild-type strain (Brenner 1974) and CB4856 served as the Hawaiian strain used for snip single-nucleotide polymorphism (SNP) mapping. The alleles used in this study are listed by linkage groups as follows:

LGI: *unc-13*(*n2813*), *unc-13*(*e312*), and *unc-13*(*e1091*) (Brenner 1974; Kohn *et al.* 2000; Yook *et al.* 2001).
LGII: *rab-3*(*js49*) (Nonet *et al.* 1997).
LGIV: *unc-24*(*e138*), *dpy-20*(*e1282*), and *unc-29*(*e193*) (Brenner 1974); *sax*-7(*eq1*) (Wang *et al.* 2005; Zhou *et al.* 2008); *sax-7*(*nj48*) (Sasakura *et al.* 2005); *juIs1* (Hallam and Jin 1998); *gtl-2*(*tm1463*) (The Japanese National Bioresource Project); and *gtl-2*(*eq3*), which was outcrossed from the LH1 strain (Wang *et al.* 2005) (see *Three-factor cross analysis* in *Materials and Methods*).
LGX: *oxIs12 (*McIntire *et al.* 1997).

The integrated *oxIs12* (P_{unc-47}::*gfp*) (McIntire *et al.* 1997), *juIs1* (P_{unc-25}::*snb-1*::*gfp*) (Hallam and Jin 1998), *evIs111* (*rgef-1*::*gfp*), and *wdIs20*(P_{unc-4}::*snb-1*::*gfp*) (Lickteig *et al.* 2001) transgenes were crossed into respective strains to visualize the architecture of the whole nervous system as well as examine GABA and cholinergic neuron and synapse morphology. The strains generated in this study are as follows:

LH202: *sax-7*(*eq1*) *gtl-2*(*eq3*) was outcrossed eight times, and the deletion was confirmed by DNA sequencing of PCR products.
LH216: *sax-7*(*eq1*) *gtl-2*(*tm1463*).
LH250: *sax-7*(*nj48*) *gtl-2*(*eq3*).
LH358: *gtl-2*(*eq3*).
LH749: *sax-7*(*nj48*) *gtl-2*(*eq3*); *oxIs12*.
LH750: *sax-7*(*eq1*) *gtl-2*(*tm1463*); *oxIs12*.
LH832: *juIs1 sax-7*(*eq1*) *gtl-2*(*tm1463*).
LH766: *unc-13*(*n2813*); *sax-7*(*eq1*).
LH981: *wdIs20*.
LH987: *sax-7*(*eq1*) *gtl-2*(*tm1463*); *wdIs20*.
LH984: *sax-7*(*eq1*); *evIs111*.
LH988: *sax-7*(*eq1*) *gtl-2*(*tm1463*); *evIs111*.
LH985: *unc-13*(*e312*); *sax-7*(*eq1*).
LH986: *unc-13*(*e1091*); *sax-7*(*eq1*).
LH989: *rab-3*(*js49*); *sax-7*(*eq1*).

Three-factor cross analysis

A three-factor cross, which was performed to test for a mutation to the right of *sax-7*, utilized the *unc-24* gene, which maps to the left of *sax-7* (positions 3.51 and 3.59, respectively), and the *dpy-20* gene, which maps ~1.6 map units to the right of *sax-7*. Crossing into the LH1 strain, we generated a strain with the genotype *unc-24 dpy-20/ sax-7(eq1)* and two classes of genetic recombinants were isolated: Unc non-Dpy and Dpy non-Unc. For each recombinant of each class, it was determined whether thin, lethargic worms were among the progeny. If these traits were conferred by *eq1*, then they would show close linkage to *unc-24* so that almost all of the Dpy non-Unc recombinants should segregate thin, lethargic worms.

Of the 30 recombinants analyzed, only 4 of 13 Dpy non-Unc recombinants segregated thin, lethargic progeny while 11 of 17 Unc non-Dpy recombinants segregated thin, lethargic progeny. These data demonstrate that LH1 has a second mutation we designated as *eq3* that maps between *unc-24* and *dpy-20* and is somewhat closer to the latter marker (Figure 1).

Molecular characterization of gtl-2 mutants

eq3 or *tm1463* homozygotes were lysed to provide template DNA for the generation of PCR products specific for the *gtl-2* gene. Primers were chosen such that the DNA sequence could be determined for all of the exons and for short regions of the introns adjoining the exons. The DNA sequence of both strands of PCR products was determined *en masse* at the Advanced Genetic Analysis Center (University of Minnesota). DNA sequences were compared with the wild-type sequence at wormbase.org. The *eq3* mutation was confirmed by sequencing wild-type DNA in the region.

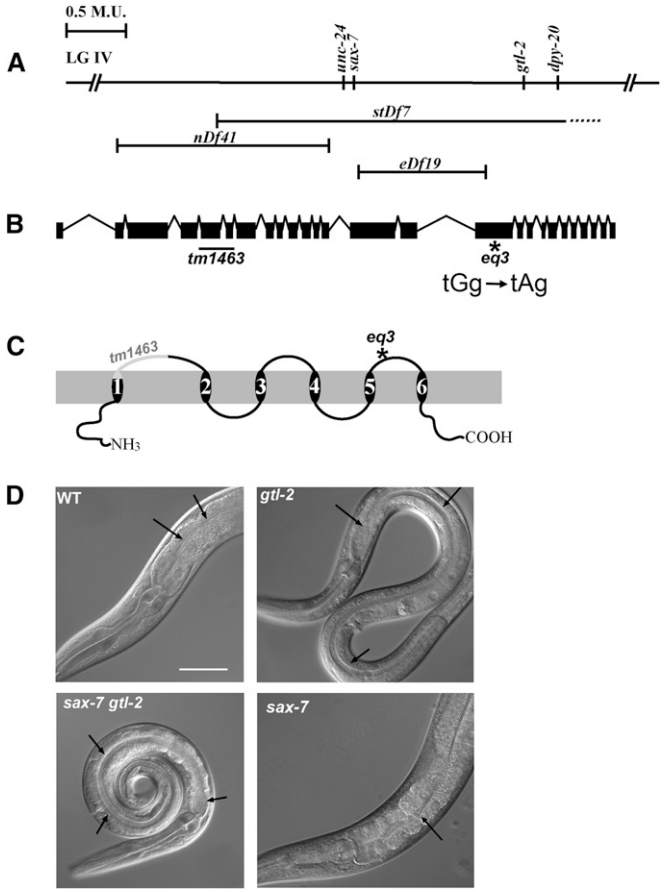

Figure 1 *sax-7* and the closely linked *gtl-2* genetically interact to produce synthetic coiling of the body. (A) The positions of *sax-7* and *gtl-2* on linkage group IV. The chromosomal deficiency *stDf7* uncovers *sax-7*, *gtl-2*, and *dpy-20*. The right breakpoint of *stDf7* is not known (dashed line). Neither *sax-7* nor *gtl-2* is uncovered by two other deficiencies in the region, *nDf41* and *eDf19*. (B) The 26 exons of *gtl-2* are represented by solid boxes. The positions of the *eq3* and *tm1463* mutations are indicated. (C) GTL-2 is predicted to have six transmembrane domains that form a pore for cations with the N and C termini depicted as being cytosolic. Also indicated are the regions of the protein that are predicted to be affected by the *eq3* or *tm1463* mutations. (D) Differential interference contrast micrographs of wild-type (WT), *sax-7 gtl-2*, *gtl-2*, and *sax-7* adult animals. Note that the scrawniness of the *gtl-2* and *sax-7 gtl-2* animals is quite apparent as they are thinner and smaller than wild-type and *sax-7* animals. In addition to being scrawny, *sax-7 gtl-2* animals also tend to coil their bodies, unlike *sax-7* or *gtl-2* animals. Arrows point to the intestinal lumen, which is enlarged in *gtl-2* and *sax-7 gtl-2* animals, indicating constipation, compared to wild-type and *sax-7* animals. Bar, 50 μm.

DNA constructs and generation of transgenic animals

Transgenic animals were generated according to standard procedures (Mello *et al.* 1991). Based on Zhou *et al.* (2008), we injected *sax-7 gtl-2* animals with co-injection marker P_{str-1}::*gfp* (Troemel *et al.* 1995) along with different *sax-7* constructs that include 70 ng/μl pLC262 (P_{sax-7}::*sax-7*) or 10 ng/μl pLC237 (P_{myo-3}::*sax-7L*) or 20 ng/μl pLC227 ($P_{unc-119}$::*sax-7L*) or 2.5 ng/μl pLC238 (P_{dpy-7}::*sax-7L*). To generate the inducible *sax-7* construct (pLC672), we inserted *sax-7L* into pPD49.78, which contains the HSP16-2 promoter (courtesy of A. Fire, Stanford University School of Medicine, Stanford, CA) between the *Bam*HI and *Kpn*I sites. pLC672 was injected at 50 ng/μl along with 1.5 ng/μl of P_{myo-2}::tdtomato as a co-injection marker:

LH416–LH418: *sax-7*(*eq1*) *gtl-2*(*tm1463*); *eqExP*$_{sax-7}$::*sax-7*.
LH419–LH421: *sax-7*(*nj48*) *gtl-2*(*eq3*); *eqExP*$_{sax-7}$::*sax-7*.
LH410–LH412: *sax-7*(*eq1*) *gtl-2*(*tm1463*); *eqExP*$_{unc-119}$::*sax-7*.
LH413–LH415: *sax-7*(*nj48*) *gtl-2*(*eq3*); *eqExP*$_{unc-119}$::*sax-7*.
LH403–LH406: *sax-7*(*eq1*) *gtl-2*(*tm1463*); *eqExP*$_{myo-3}$::*sax-7*.
LH407–LH409: *sax-7*(*nj48*) *gtl-2*(*eq3*); *eqExP*$_{myo-3}$::*sax-7*.
LH422–LH423: *sax-7*(*eq1*) *gtl-2*(*tm1463*); *eqExP*$_{dpy-7}$::*sax-7*.
LH488–LH490: *sax-7*(*nj48*) *gtl-2*(*eq3*); *eqExP*$_{dpy-7}$::*sax-7*.
LH957–LH960: *unc-13*(*n2813*); *sax-7*(*eq1*); *eqExP*$_{hsp16.2}$::*sax-7*.

The cosmid F54D1 was injected at 5 ng/μl together with 100 ng/μl pTG96 (Yochem *et al.* 1998) into *gtl-2* animals to generate *eqEx72*, which was used for mosaic analysis (see *Materials and Methods*).

P_{gtl-2}::*gtl-2* (pLC645): A 17.5-kb *Xma*I–*Kpn*I fragment from cosmid F54D1 was subcloned into pBS II SK−. This fragment consists of 6.4 kb upstream of the putative ATG start codon and 347 bp downstream from the poly(A) addition site of the gene (Figure 1). A total of 50 ng/μl pLC pLC645 was injected along with 70 ng/μl P_{str-1}::*gfp* into *sax-7 gtl-2* animals.

P_{gtl-2}::*gtl-2*::*gfp* (pLC646): GFP DNA PCR'd from pPD95.75 was inserted in frame into pLC645 into a *Not*I site that was engineered upstream of the stop codon of *gtl-2* DNA. *gtl-2* animals injected with 30 ng/μl pLC646 along with 70 ng/μl of co-injection marker pRF4 (Mello *et al.* 1991) were rescued as were *sax-7 gtl-2* transgenic animals injected with 20 ng/μl pLC646 along with 2 ng/μl of co-injection marker P_{myo-2}::tdtomato.

To generate tissue-specific-expressing *gtl-2* constructs, tissue-specific promoters were PCR'd and put in frame of (1) pLC606, a derivative of pLC645 that lacks the *gtl-2* promoter, or (2) pLC607, a derivative of pLC646 that lacks the *gtl-2* promoter. For expression in the excretory cell, we generated P_{exc-5}::*gtl-2* (pLC611) and P_{exc-5}::*gtl-2*::*gfp* (pLC623); both constructs contain 2.6 kb of sequence upstream of the putative *exc-5* start codon (Suzuki *et al.* 2001). A total of 50 ng/μl or 20 ng/μl of the *gtl-2* constructs was injected along with 2 ng/μl of co-injection marker P_{myo-2}::tdtomato into *sax-7 gtl-2* or *gtl-2* animals. For expression in hyp7, we generated P_{dpy-7}::*gtl-2* (pLC612) and P_{dpy-7}::*gtl-2*::*gfp* (pLC631); both constructs contain 400 bp of sequence upstream of the putative *dpy-7* start codon (Gilleard *et al.* 1997). A total of 2.5 ng/μl of the *gtl-2* constructs was injected along with 70 ng/μl of co-injection marker P_{str-1}::*gfp* into *sax-7 gtl-2* animals. For expression in body-wall muscles, we generated P_{myo-3}::*gtl-2* (pLC613) and P_{myo-3}::*gtl-2*::*gfp* (pLC637); both constructs contain 2.3 kb *myo-3* promoter sequence (Okkema *et al.* 1993). A total of 20–50 ng/μl of each construct was injected along 70 ng/μl of co-injection marker P_{str-1}::*gfp* into *sax-7 gtl-2* or *gtl-2* animals. For expression in the nervous system, we

generated P_{rgef-1}::*gtl-2* (pLC626) and P_{rgef-1}::*gtl-2*::*gfp* (pLC639); both constructs contain 3.5 kb of *rgef-1* promoter sequence (Altun-Gultekin *et al.* 2001). A total of 20–40 ng/μl of the *gtl-2* constructs was injected along with 70 ng/μl or 2 ng/μl of co-injection markers P_{myo-2}::tdtomato into *sax-7 gtl-2* animals:

LH530–LH532: *sax-7*(*eq1*) *gtl-2*(*tm1463*); *eqExP*$_{gtl-2}$::*gtl-2*.
LH694–LH696: *sax-7*(*eq1*) *gtl-2*(*tm1463*); *eqExP*$_{gtl-2}$::*gtl-2*::*gfp*.
LH491–LH493: *sax-7*(*eq1*) *gtl-2*(*tm1463*); *eqExP*$_{exc-5}$::*gtl-2*.
LH505–LH506: *sax-7*(*eq1*) *gtl-2*(*tm1463*); *eqExP*$_{dpy-7}$::*gtl-2*.
LH507–LH509: *sax-7*(*eq1*) *gtl-2*(*tm1463*); *eqExP*$_{myo-3}$::*gtl-2*.
LH659–LH660: *sax-7*(*eq1*) *gtl-2*(*tm1463*); *eqExP*$_{rgef-1}$::*gtl-2*.

Genetic mosaic analysis

Genetic mosaics can be analyzed in *C. elegans* on the basis of the occasional failure of an extrachromosomal array to disjoin during embryonic cell divisions Yochem *et al.* 1998. The source of the mosaics was LH104 [*gtl-2(eq3)*; *eqEx72[gtl-2(+)*; *sur-5*::*gfp]*], a strain having an extrachromosomal array that contains copies of cosmid clone F54D1, which efficiently rescues mutant, chromosomal copies of *gtl-2*, and copies of the plasmid pTG96, for nuclear expression of SUR-5::GFP in many cell types (Yochem *et al.* 1998). Thus, *gtl-2(+)* and nuclear green fluorescence cosegregate in these strains. Progeny of the strains were examined with a dissecting microscope equipped for epifluorescence for those lacking SUR-5::GFP in some but not all cells, indicating nondisjunction of the array during development. The embryonic cell division at which the nondisjunction occurred was deduced on the basis of the anatomy and nearly invariant cell lineage (Sulston *et al.* 1983) following an examination of the mosaics with a compound microscope.

Whole-mount immunofluorescence

Young adult animals of wild-type and *sax-7*(*eq1*) *gtl-2* (*eq3*) backgrounds were fixed in methanol and stained for indirect immunofluorescence, using the freeze-crack methanol fixation method. Fixed animals were washed, incubated with primary antibodies anti-UNC-17 (1:2000) and anti-UNC-29 (1:100) at 4°, washed again, and incubated in secondary antibody (Alexa 488 and 568; Molecular Probes, Eugene, OR) for 2 hr at room temperature. After washing, the samples were mounted and examined using an Axioplan 2 microscope (Carl Zeiss, Thornwood, NY). Images were acquired using the AxioCam MRM and AxioVision 4.5 software (Carl Zeiss).

Live-animal microscopy

Nervous system architecture was examined in animals containing the *evIs111* and *oxIs12* GFP markers while synapse morphology in GABA and cholinergic neurons was examined in animals containing the *juIs1* and *wdIs20* GFP markers, respectively. Synchronized L4 or young adult animals were mounted on 2% agarose pads and anesthetized using 1% (v/v) 1-phenoxy-2-propanol in M9 buffer and scored for defects, using an Axioplan 2 microscope (Carl Zeiss). Images of nervous system architecture in animals containing *evIs111* were collected as stacks along the *z*-axis, using an Olympus Fluoview FV1000 upright confocal microscope and Fluoview software. Images of the other animals were acquired using an AxioCam MRM and AxioVision 4.5 software (Carl Zeiss). Displaced neurons were scored as previously described (Zhou and Chen 2011). To quantitate defects in synapse formation, images of the dorsal nerve cord were acquired and synaptic puncta were analyzed manually over 50 μm. $n = 25$ animals for each strain.

Aldicarb and Levamisole assays

The assays are based on previously established protocols (Miller *et al.* 1996; Saifee *et al.* 1998). Young adults were placed onto NGM plates containing either 0.25 mM Levamisole (≥99% tetramisole hydrochloride; Sigma-Aldrich) or 0.75, 1, 1.25, or 1.5 mM of the acetylcholinesterase inhibitor Aldicarb (Aldicarb Pestanal; Sigma-Aldrich). At 30-min intervals for 2.5–3 hr, we counted the number of paralyzed animals *vs.* animals that exhibited locomotion after being prodded with a platinum wire. For each strain, we performed 10–12 assays, in which $n = 25$ animals in each assay.

Growth on varying amounts of magnesium supplementation

gtl-2 and *sax-7 gtl-2* L4-staged animals were placed in NGM plates containing 0, 1, 2, or 4 mM magnesium supplementation. Their progeny were examined for differences in growth, movement, and Aldicarb sensitivity. Aldicarb assays were performed as described, except the plates used were NGM containing Mg^{2+} supplementation that corresponded to that of their growth medium.

Thrashing assays

The thrashing assays were performed as previously described (Miller *et al.* 1996). Young adult hermaphrodites were transferred into a well of a depression slide containing 200 μl M9 buffer. After 2 min of recovery, the number of times an animal thrashed (bending at midbody) was counted for 1 min. $n = 50$ animals per strain.

Heat-shock induction of sax-7 expression

All strains were cultured at 15° to reduce potential leakiness of the *hsp16.2* promoter. L4-staged or young adult transgenic and nontransgenic control animals were transferred and incubated at 34° for 2 hr before they were allowed to recover at 15° for either 3 or 15 hr. After recovery, animals were subjected to the Aldicarb assay (post-heat-shock recovery time of 3 hr), the thrashing assay (post-heat-shock recovery time of 15 hr), or examination of the displaced neuron phenotype (post-heat-shock recovery time of 3 and 15 hr).

Results

eq3 is a mutation in the gtl-2 gene

The LH1 strain, which is homozygous for the *sax-7* deletion allele, *eq1*, was previously described as having a phenotype that is more severe than reported for other *sax-7* alleles. In

addition to the neuronal position maintenance defects observed in other *sax-7* mutant backgrounds, LH1 animals are also scrawny, slow growing (Gro), egg-laying defective (Egl), constipated (Con), and lethargic with a tendency to coil their bodies, behaviors that are not exhibited by other *sax-7* alleles (Wang *et al.* 2005). One possible explanation for this difference is that *eq1*, unlike the other *sax-7* alleles, is a null mutation, as revealed by molecular and genetic analyses and the lack of detectable SAX-7 protein in *sax-7*(*eq1*) animals immunostained with an anti-SAX-7 antibody; in contrast, the other *sax-7* alleles still show residual SAX-7 protein (Zhou *et al.* 2008). An alternative explanation is the presence of a second mutation that remained linked to *sax-7* after the original isolation and outcrossing of the *eq1* mutation. Indeed, examination by three-factor crosses (see *Materials and Methods*) revealed a second mutation, designated as *eq3*, to the right of *sax-7* in the LH1 strain (Figure 1A). Free of *eq3*, the *sax-7(eq1)* phenotype is generally similar to that described for other *sax-7* alleles, including defective neuronal position maintenance (Sasakura *et al.* 2005; Zhou *et al.* 2008). The scrawny, Gro, Egl, Con, and lethargic phenotype of LH1 is attributed to the *eq3* mutation (Figure 1D).

Using SNPs present in a Hawaiian strain of *C. elegans*, we mapped the *eq3* mutation relative to the physical map (Davis *et al.* 2005). Micro-injection of the F54D1cosmid clone within the mapped interval conferred full rescue of *eq3*. Further subcloning and PCR analysis of F54D1, together with DNA sequencing of mutant homozygotes, demonstrated that *eq3* is a mutation in *gtl-2*, which encodes a member of the TRPM family of channels that regulate the passage of divalent cations, including Mg^{2+} and Ca^{2+} (Venkatachalam and Montell 2007; Teramoto *et al.* 2010; Nilius and Owsianik 2011).

eq3 is a G-to-A transition that changes amino acid 1064 from a tryptophan to an amber stop, which should result in a truncation of the product in the third extracellular loop (Figure 1, B and C). *gtl-2(eq3)* homozygotes are indistinguishable from animals homozygous for *gtl-2(tm1463)*, a previously described loss-of-function deletion allele (Stawicki *et al.* 2011). In addition to the Gro, Egl, and lethargic phenotype, animals homozygous for *eq3* or *tm1463* are also Con and scrawny, phenotypes that are apparent in Figure 1D. These phenotypes are similar to those of *eq3/tm1463 trans*-heterozygotes as well as *eq3/stDf7* or *tm1463/stDf7* hemizygotes, where *stDf7* is a chromosomal deficiency that removes multiple genes, including *gtl-2* (Figure 1A).

gtl-2 genetically interacts with the cell-adhesion gene sax-7

Unlike the other described phenotypes, the tendency to coil by LH1 animals is not displayed by either *sax-7*(*eq1*) or *gtl-2*(*eq3*) single-mutant animals (Figure 1D). This synthetic coiling phenotype is also exhibited by additional *sax-7 gtl-2* strains we generated with *gtl-2*(*tm1463*) and another putative null *sax-7* allele, *nj48*. Thus the synthetic coiling in LH1 is not allele specific, indicating *sax-7* and *gtl-2* genetically interact.

To determine the significance of this genetic interaction, *i.e.*, the cause of the coiling phenotype, we first examined *sax-7 gtl-2* nervous system morphology. Other than the *sax-7*-related neuronal displacement, we detected no obvious abnormalities in nervous system architecture, as visualized by a previously established neuronally-expressed GFP marker, *evIs111*. In addition, we did not detect any significant difference in synapse morphology and spacing, as visualized by synaptobrevin/SNB-1::GFP in both cholinergic and GABAergic neurons (Supporting Information, Figure S1). These results suggest the coiling phenotype is not a result of defects in nervous system architecture or development; rather, this coiling phenotype is more likely due to impaired nervous system function. Indeed, animals with impaired neuromuscular function can exhibit coiling phenotypes (Rand and Russell 1984; Alfonso *et al.* 1994; Harris *et al.* 2000). Moreover, *gtl-2* was recently shown to have modulatory effects on excitation–inhibition synaptic imbalance caused by increased activity in the neuronal ACR-2R acetylcholine receptor (Stawicki *et al.* 2011). We thus hypothesized that *sax-7 gtl-2* animals might have abnormal neuromuscular function.

To test this hypothesis, we assessed whether *sax-7 gtl-2* animals might show resistance to Aldicarb, a cholinesterase inhibitor that has been used to successfully identify synaptic transmission mutants (Nguyen *et al.* 1995; Miller *et al.* 1996; Sieburth *et al.* 2005). Exposure to cholinesterase inhibitors causes acute paralysis in wild-type animals as a result of acetylcholine accumulation at neuromuscular junctions. However, mutants with impaired acetylcholine secretion or acetylcholine receptor function generally exhibit the **r**esistance to **i**nhibitors of **c**holinesterase (Ric) phenotype. We performed a time-course response to four different Aldicarb concentrations. While the different strains exhibited consistent responses in all conditions tested, the 2-hr time point on 1 mM Aldicarb provided the highest sensitivity to changes in the animals' response (Figure 2A). A total of 5–7% of *sax-7* animals and 10% of *gtl-2* animals still exhibited movement by 2 hr of exposure to 1 mM Aldicarb; by comparison, >30% of *sax-7 gtl-2* animals were still able to move (Figure 2B), thus displaying a level of Aldicarb resistance that is synergistic rather than additive. As expected, virtually no wild-type animals were moving, while 100% of *unc-29* animals, which are deficient in nicotinic acetylcholine receptor function (Fleming *et al.* 1997), were still active and exhibiting a strong level of Aldicarb resistance (data not shown). The *sax-7 gtl-2* Aldicarb resistance can be reduced with transgenic expression of *gtl-2* or *sax-7* (Figure 2B). The synthetic coiling and synergistic Ric phenotypes by *sax-7 gtl-2* animals relative to each single-mutant background reveal a genetic interaction between *sax-7* and *gtl-2* and suggest that the loss of function of both genes results in abnormal neuromuscular function.

sax-7 gtl-2 Aldicarb resistance and coiling behavior is suppressed by nonneuronal gtl-2 expression or growth on culture medium with reduced Mg^{2+} levels

To determine how loss of *gtl-2* contributes to *sax-7 gtl-2* synthetic phenotypes, we examined the site of action for GTL-2,

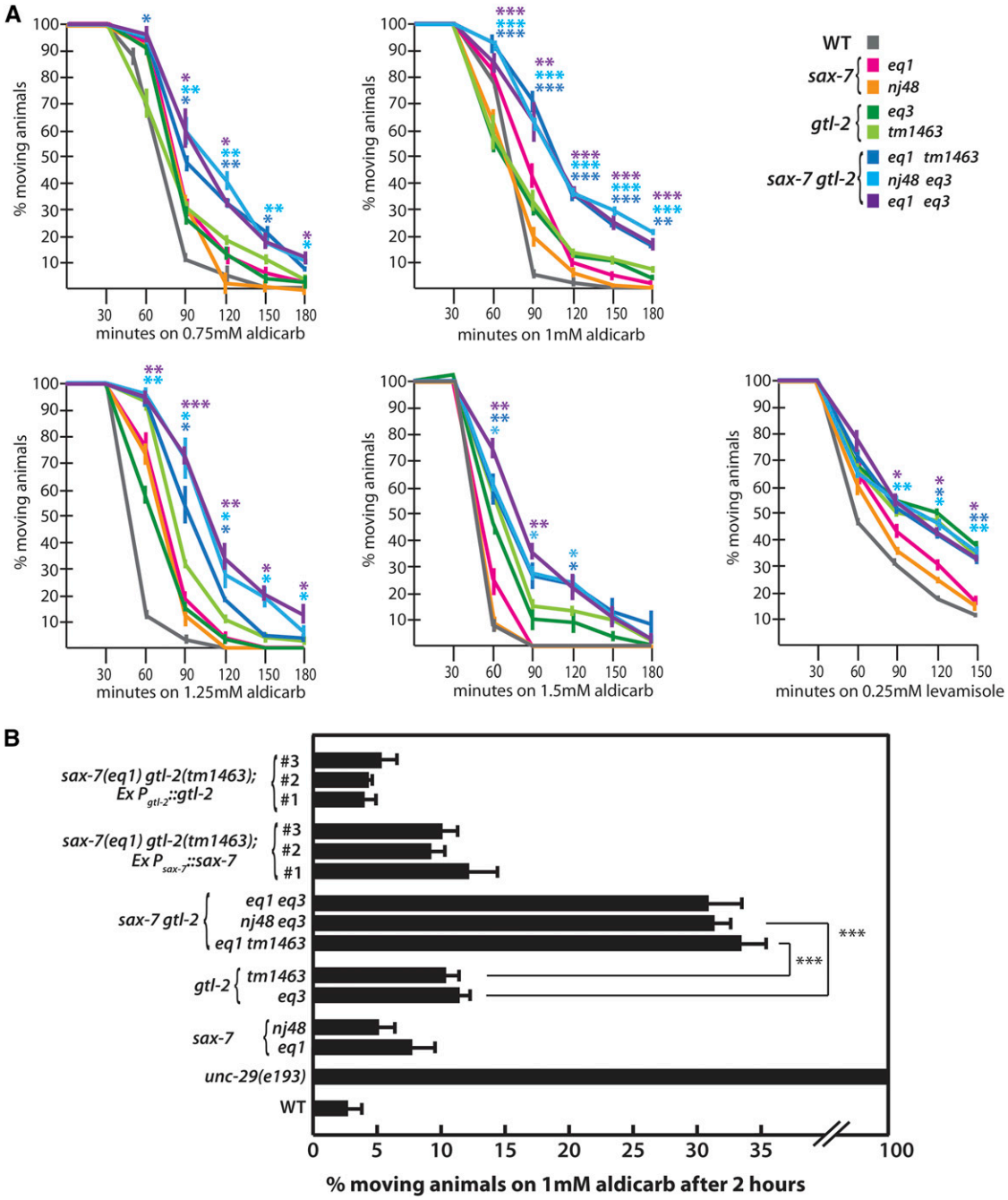

Figure 2 The response of *sax-7 gtl-2* as well as *sax-7* and *gtl-2* single-mutant strains to the cholinesterase inhibitor, Aldicarb, and the acetylcholine receptor agonist, Levamisole. (A) A time-course response of wild-type and mutant strains on NGM media containing 0.75, 1, 1.25, or 1.5 mM Aldicarb and 0.25 mM Levamisole. Controls include wild type (WT), which is sensitive to Aldicarb and Levamisole, and *unc-29*(*e193*), which is resistant to Aldicarb and Levamisole (data not shown) (Miller *et al.* 1996; Fleming *et al.* 1997). The color-coded *'s in the Aldicarb assays represent the *P*-values calculated by Student's *t*-test comparing *sax-7 gtl-2* Aldicarb resistance to the corresponding *gtl-2* allele. On the other hand, the color-coded *'s in the Levamisole assays represent the *P*-values when comparing *sax-7 gtl-2* Levamisole resistance to the corresponding *sax-7* allele. $*P < 0.05$, $**P < 0.005$, $***P < 0.0001$. (B) The percentage of animals moving after a 2-hr exposure to 1 mM Aldicarb. Transgenes containing wild-type *gtl-2* can consistently suppress the Aldicarb resistance exhibited by *sax-7 gtl-2* double mutants. Similarly, transgenes containing wild-type *sax-7* restore the level of resistance of the double mutant to that of the *gtl-2* single mutant. Three independent transgenic lines were analyzed for each construct assessed. Error bars show the standard error of the mean of at least 12 sample sets, where $n = 25$ animals for each set.

using tissue-specific *gtl-2* expression and mosaic analysis. The GTL-2 TRPM channel was previously shown to be expressed in the excretory cell and hyp7 (Teramoto *et al.* 2010; Stawicki *et al.* 2011). In agreement with our mosaic analysis (Figure S2), expression of *gtl-2*::*gfp* in either of these tissues suppressed the *sax-7 gtl-2* coiling tendency and *gtl-2*-related behavioral phenotypes such that transgenic *sax-7 gtl-2* double-mutant animals are healthy and robust, exhibiting relatively normal

movements. Importantly, Aldicarb resistance in these transgenic *sax-7 gtl-2* animals is suppressed (Figure 3A). In contrast, *gtl-2*::*gfp* expressed in body-wall muscle or neurons did not suppress *sax-7 gtl-2* coiling and Ric phenotypes. The ability for nonneuronal *gtl-2* expression to suppress the apparent neuromuscular defects is consistent with a recent study that showed similar *gtl-2* expression in either of these nonneuronal tissues can also modulate ACR-2-related synaptic activity (Stawicki *et al.* 2011).

GTL-2 plays a significant role in maintaining systemic Mg^{2+} levels; indeed, *gtl-2* mutant animals are hypermagnesemic (Teramoto *et al.* 2010). Because hypermagesemia can affect synaptic transmission to cause neurologic symptoms (Topf and Murray 2003), we hypothesized that the increased systemic Mg^{2+} level caused by loss of *gtl-2* function contributes to the coiling and Ric phenotype in *sax-7 gtl-2* animals. To test this hypothesis, we assessed the effects of culturing *sax-7 gtl-2* animals on *C. elegans* growth medium (NGM) supplemented with different amounts of Mg^{2+} on movement and response to aldicarb. *sax-7 gtl-2* animals cultured on standard NGM, which is supplemented with 1 mM Mg^{2+}, display the described phenotypes and Aldicarb resistance (Figure 1 and Figure 2). But when cultured on nonsupplemented NGM [nonsupplemented NGM still contains some residual Mg^{2+} due to its presence in the bacteria fed to *C. elegans* as well as the agar used in NGM (Teramoto *et al.* 2010)], *sax-7 gtl-2* animals are robust and healthy, exhibiting minimal coiling behavior and importantly, no significant resistance to Aldicarb (Figure 3B). Aldicarb responses were not assessed under conditions of higher levels of Mg^{2+} (2 and 4 mM) because the already slow growth of the *sax-7 gtl-2* and *gtl-2* mutant animals on standard NGM was further impaired at these higher concentrations (data not shown) (Teramoto *et al.* 2010), making it difficult to obtain sufficient numbers of adult animals to perform the Aldicarb response assay. Thus reducing Mg^{2+} levels in the culture medium effectively suppressed the *sax-7 gtl-2* coiling and Ric phenotypes, consistent with the idea that these phenotypes are due, in part, to a systemic increase in Mg^{2+}.

Tissue-specific suppression of Aldicarb resistance reveals a requirement for sax-7 in neurons

Resistance to Aldicarb is observed in animals with impaired presynaptic or postsynaptic function (Nguyen *et al.* 1995; Miller *et al.* 1996; Sieburth *et al.* 2005). Because *sax-7* is widely expressed (Chen *et al.* 2001; Wang *et al.* 2005), the *sax-7 gtl-2* Ric phenotype may result from a loss of *sax-7* function in neurons and/or muscles or other tissues. Indeed, *sax-7* was previously shown to be required predominantly in neurons but also in the adjacent body-wall muscles and hypodermis for optimal maintenance of motor neuron positions (Wang *et al.* 2005). We thus assessed the level of Aldicarb resistance in *sax-7 gtl-2* animals expressing *sax-7* in each of the three tissues, using the *unc-119*, *myo-3*, or *dpy-7* promoters (Okkema *et al.* 1993; Gilleard *et al.* 1997; Altun-Gultekin *et al.* 2001). *sax-7* expression in neurons suppressed the *sax-7 gtl-2* aldicarb resistance equally as well as

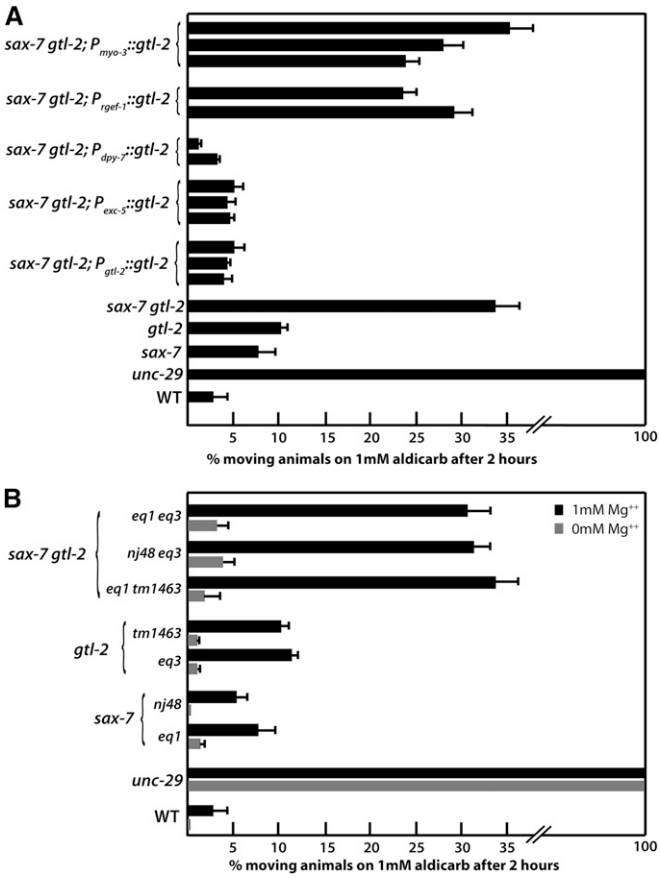

Figure 3 The *sax-7 gtl-2* Ric phenotype can be suppressed with nonneuronal *gtl-2* expression and culturing of mutant animals on media with reduced Mg^{2+} levels. (A) Expression of wild-type *gtl-2* driven in hyp7 or in the excretory cell by the *dpy-7* and *exc-5* promoters, respectively, can suppress the *sax-7 gtl-2* Aldicarb resistance just as well as the *gtl-2* gene. In contrast, *gtl-2* expressed in neurons or muscle by the *unc-119* and *myo-3* promoters, respectively, cannot suppress the *sax-7 gtl-2* Ric phenotype. Two to three independent transgenic lines were analyzed for each construct assessed. The rescue abilities of these constructs were similar in all *sax-7 gtl-2* backgrounds but only data for the *sax-7*(*eq1*) *gtl-2*(*tm1463*) background are shown. (B) The Ric phenotype exhibited by *sax-7 gtl-2* animals cultured on standard NGM, which is supplemented with 1 mM Mg^{2+}, is dramatically suppressed when animals are cultured on NGM lacking Mg^{2+} supplementation. Error bars show the standard error of the mean of at least 12 sample sets, where $n = 25$ for each set.

full-length genomic *sax-7* (Figure 4). In contrast, *sax-7* expression in body-wall muscles or the hypodermis failed to suppress the resistance.

The ability for neuronal but not body-wall muscle expression of *sax-7* to suppress the *sax-7 gtl-2* Ric phenotype is consistent with a neuronal role for *sax-7*. To test this hypothesis, we assayed responses of the mutant strains to the nicotinic acetylcholine receptor agonist, Levamisole. Wild-type animals exposed to Levamisole become paralyzed due to continued stimulation of body-wall muscles, which are enriched with acetylcholine receptors; in contrast, animals with defective postsynaptic acetylcholine receptor functions show resistance to Levamisole (Lewis *et al.* 1980;

Miller *et al.* 1996; Fleming *et al.* 1997). After 2.5 hr of exposure to 0.25 mM Levamisole, *sax-7* animals responded similarly to wild-type animals, with most animals paralyzed and only 12–15% animals still moving. By comparison, *gtl-2* and *sax-7 gtl-2* animals showed similar responses, with 32–38% of animals still mobile (Figure 2A). As expected, *unc-29* mutant animals, which have impaired acetylcholine receptor function, are resistant to Levamisole (data not shown) (Fleming *et al.* 1997). The comparable Levamisole resistance levels of *gtl-2* and *sax-7 gtl-2* animals indicate that loss of *sax-7* function does not contribute to the *sax-7 gtl-2* Levamisole resistance. Taken together, these results support a neuronal role for *sax-7* that can impinge on synaptic function.

Transient, late-onset sax-7 expression rescues sax-7 gtl-2 Aldicarb resistance but not neuronal displacement, revealing a novel nondevelopmental role for sax-7

sax-7 mutant animals display progressive displacement of different neurons, including cholinergic and GABA motor neurons (Wang *et al.* 2005; Zhou *et al.* 2008). Yet *sax-7* single-mutant animals display generally wild-type locomotion and sensitivity to Aldicarb. How does loss of *sax-7* contribute to the synthetic *sax-7 gtl-2* phenotypes? One possible explanation is the *sax-7*-related neuronal displacement may modestly impair nervous system function to an undetectable level, but when combined with minor *gtl-2*-related abnormalities in synaptic function, becomes significantly compromised. Alternatively, *sax-7* may possess an as-yet-uncharacterized, direct role in synaptic regulation that can be detected only in sensitized backgrounds. To test this possibility, we expressed *sax-7*, using an inducible heat-shock promoter in *sax-7 gtl-2* L4-staged larvae or young adults after the peak of neuronal displacement (Wang *et al.* 2005). A 2-hr induction of the transgene at an elevated temperature of 34°, followed by a 3-hr recovery period at 15°, significantly reduced the level of *sax-7 gtl-2* Aldicarb resistance (Figure 6A). However, the same *sax-7* induction did not rescue the neuronal displacement phenotype (Figure 6C). We conclude that neuronal displacement is not the underlying cause of the *sax-7 gtl-2* Ric phenotype. Moreover, because of the ability for a late-onset and transient *sax-7* expression to rescue the Ric phenotype, we infer that the *sax-7 gtl-2* Ric phenotype is caused by functional, not developmental defects. Taken together, these results reveal a novel nondevelopmental role for *sax-7* in neurons that can modulate synaptic function.

sax-7 genetically interacts with unc-13 and rab-3, genes that function in neurotransmission

To further investigate the hypothesis that *sax-7* modulates synaptic function, we probed whether *sax-7* genetically interacts with the core pathway of genes essential for neurotransmitter release. Loss-of-function alleles in these genes generally result in severe locomotion defects, severely abnormal aldicarb responses, and sometimes lethality (Saifee *et al.* 1998; Kohn *et al.* 2000), making it difficult to detect

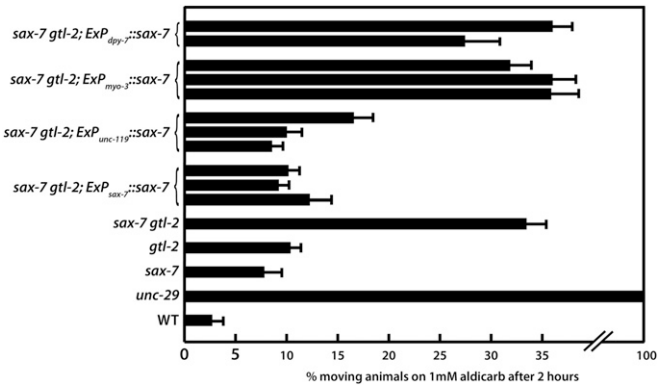

Figure 4 Rescue of the *sax-7 gtl-2* Ric phenotype with tissue-specific *sax-7* expression reveals a requirement for *sax-7* in neurons. Neuronal expression of *sax-7* by the *unc-119* promoter suppresses *sax-7 gtl-2* resistance to Aldicarb to the same level as that of the full-length *sax-7* gene, unlike *sax-7* expression in body-wall muscle or hyp7. Three independent transgenic lines were analyzed for each construct assessed. The rescue abilities of these constructs are similar in all *sax-7 gtl-2* strains. For simplicity, only data for the *sax-7*(*eq1*) *gtl-2*(*tm1463*) background are shown. Error bars show the standard error of the mean of at least 12 sample sets, where $n = 25$ for each set.

potential genetic interactions with *sax-7*. To bypass this difficulty, we took advantage of a fortuitous missense mutation (*n2813*) in *unc-13*, which was previously used as a sensitized background to successfully identify and study genes involved in synaptic transmission (Yook *et al.* 2001). While *unc-13* is essential for synaptic vesicle exocytosis and thus neurotransmitter release, *unc-13*(*n2813*) homozygous animals, like *sax-7* null animals, move relatively well and are difficult to distinguish from wild-type animals (Kohn *et al.* 2000; Yook *et al.* 2001). In contrast, *unc-13*(*n2813*); *sax-7* double-mutant animals barely move, showing uncoordinated and poor locomotion only when prodded, consistent with a proposed synaptic role for *sax-7*. We quantitated *unc-13*; *sax-7* movements relative to those of single-mutant animals via a body thrashing assay, which examines the thrashing locomotion behavior of animals placed in liquid (Miller *et al.* 1996) (also see *Materials and Methods*). Compared to wild-type animals, which exhibit a thrash rate of 152.44 ± 6.9 thrashes per minute, *unc-13* and *sax-7* single-mutant animals show reduced thrash rates that are 81.7% and 52.4% of wild-type rates, respectively (Figure 5A). By comparison, the thrash rate of *unc-13*(*n2813*); *sax-7* double-mutant animals is only 10.4% of the wild-type rate. The *sax-7* genetic interaction with *unc-13* is not specific to the *n2813* allele, since loss of *sax-7* also decreases the thrash rate of animals homozygous for a more severe hypomorphic *unc-13* allele, *e312* (Kohn *et al.* 2000), from 7.7 to 1.2% of the wild-type rate (Figure 5A). Loss of *sax-7* does not reduce the already diminished thrash rate of the severe loss-of-function *unc-13*(*e1091*) allele (Figure 5A).

The striking synergy observed in *unc-13*(*n2813*); *sax-7* animals afforded us a sensitive system to assess whether transient *sax-7* expression could rescue the low thrash rates

in *unc-13*; *sax-7* animals. Using the aforementioned inducible heat-shock *sax-7* transgenic system, we determined that late-onset transient *sax-7* expression could significantly recover the thrash rate in *unc-13*(*n2813*); *sax-7* L4-staged animals (Figure 6B), even as the neuronal displacement phenotype was not rescued (Figure 6C). This result indicates that the altered nervous system architecture does not contribute to the *unc-13*(*n2813*); *sax-7* locomotion phenotype and points to a nondevelopmental role for *sax-7* that impinges on synaptic function.

The RAB-3 GTPase functions in targeting the synaptic vesicle to the presynaptic density but is not a core factor that is essential for neurotransmission, unlike UNC-13 (Nonet *et al.* 1997; Gracheva *et al.* 2008). Indeed, in addition to mild behavioral defects, *rab-3*(*js49*) null animals also exhibit modest resistance to Aldicarb (Nonet *et al.* 1997), thus providing a sensitive platform to further evaluate a role for *sax-7* in modulating synaptic signaling. We first assessed whether loss of *sax-7* caused a synthetic movement phenotype in *rab-3*(*js49*) animals. While *rab-3* or *sax-7* single-mutant animals move relatively well, *rab-3*; *sax-7* animals exhibit uncoordinated, kinked, and sluggish movements. This synthetic movement defect is reflected in the low thrash rate in *rab-3*; *sax-7* animals of 33.8 ± 2.7 thrashes per minute, which is 22.2% of the wild-type thrash rate as compared to *rab-3* animals, which display 133 ± 3.8 thrashes per minute or 87.3% of the wild-type thrash rate (Figure 5A).

How does loss of both *rab-3* and *sax-7* result in the synthetic movement defects? Unlike the *unc-13* alleles we examined, which all exhibit severely Ric phenotypes (Kohn *et al.* 2000; Yook *et al.* 2001), loss of *rab-3* results only in a modest Ric phenotype that allows us to use the Aldicarb sensitivity assay as a way to assess whether the synthetic *rab-3*; *sax-7* movement defects are a result of abnormal neurotransmission. We observed that loss of *sax-7* function reduced *rab-3* Aldicarb sensitivity so that 55.6% of *rab-3*; *sax-7* animals were still moving after 3 hr of exposure to 1 mM Aldicarb, in contrast to the 11.2% of *rab-3* and 3.6% of *sax-7* animals that still showed movement (Figure 5B). Taken together, these results point to abnormal synaptic function as a contributing factor for the synthetic movement defects and enhanced Ric phenotype in *rab-3*; *sax-7* animals, adding support to the hypothesis that *sax-7* has a previously uncharacterized function that can modulate synaptic activity.

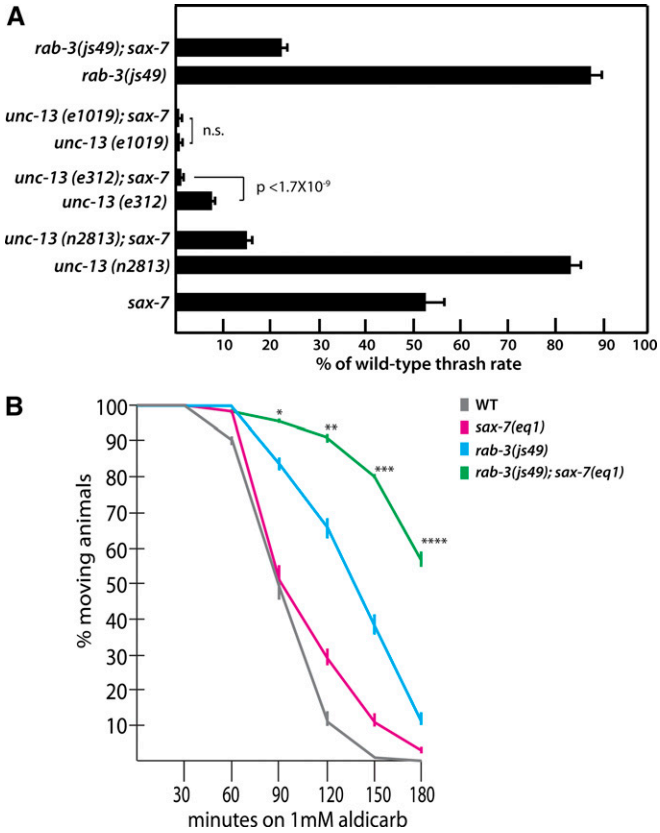

Figure 5 sax-7 genetically interacts with the neurotransmission genes, *unc-13* and *rab-3*. (A) Quantitation of locomotion defects in *unc-13*; *sax-7*, *rab-3*; *sax-7*, and the corresponding single-mutant backgrounds via the thrashing assay, where the thrash rate (number of thrashes per minute) is represented as a percentage of the wild-type thrashing rate, which is 152.44 ± 6.9 thrashes per minute. Error bars show the standard error of the mean. n = 50 animals. Error bars show the standard error of the proportion of at least 12 sample sets, where n = 25 for each set. n.s., not significant. (B) A time-course response of wild-type and mutant strains on NGM media containing 1 mM Aldicarb. Controls include wild type (WT), which is sensitive to Aldicarb, and *unc-29*(*e193*), which is resistant to Aldicarb (data not shown) (Miller *et al.* 1996). Error bars show the standard error of the mean of 10 sample sets, where n = 25 animals for each set. *'s represent the P-values calculated by Student's t-test, comparing *rab-3*; *sax-7* Aldicarb resistance to that of *rab-3*. *$P < 0.005$, **$P < 0.0005$, ***$P < 5 \times 10^{-5}$, ****$P < 5 \times 10^{-7}$.

Discussion

This study reports the identification of the *eq3* mutation in *gtl-2* in the LH1 strain that accounts for the behavioral phenotypes that are not exhibited by other *sax-7* alleles. The vicinity to and genetic interaction with *sax-7* initially obscured the presence of the *eq3* mutation in LH1. The genetic interaction between *sax-7* and *gtl-2* is manifested as a synthetic coiling behavior and Aldicarb resistance, phenotypes that are suggestive of abnormal synaptic activity. Consistent with a role in regulating synaptic function, *sax-7* also genetically interacts with *unc-13* and *rab-3*, resulting in synthetic movement defects and also enhanced Ric phenotype in *rab-3*; *sax-7* animals. Because the synthetic phenotypes of *sax-7 gtl-2* and *unc-13*(*n2813*); *sax-7* animals can be suppressed by late-onset transient expression of *sax-7*, we conclude that *sax-7* has a novel nondevelopmental role that can modulate synaptic function.

Effects of systemic magnesium homeostasis on neuromuscular activity

How does the loss of *gtl-2* function contribute to *sax-7 gtl-2* synthetic phenotypes? The *gtl-2* Gro phenotype was previously shown to be a result of the increased systemic Mg^{2+}

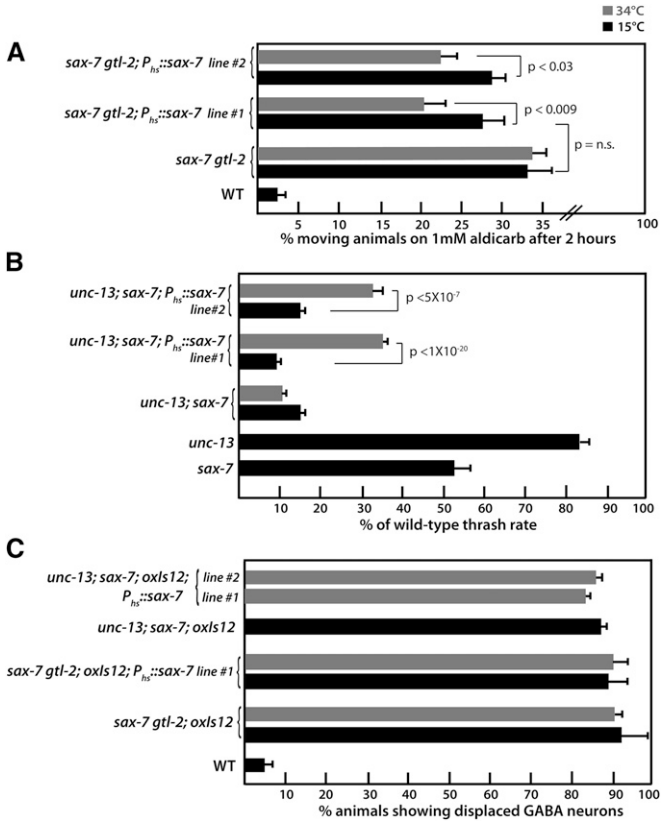

Figure 6 The synthetic phenotypes displayed by *sax-7 gtl-2* and *unc-13*; *sax-7* animals are suppressed by late-onset, transient *sax-7* expression. (A) Induced *sax-7* expression with a heat-shock promoter in young adults suppresses the Aldicarb resistance in *sax-7*(*eq1*) *gtl-2*(*tm1463*) animals. Two independent transgenic lines were assessed. Error bars show the standard error of the proportion of at least 12 sample sets, where n = 25 for each set. (B) Quantitation of locomotion defects in *unc-13*(*n2813*); *sax-7* and corresponding single-mutant backgrounds via the thrashing assay, where the thrash rate (number of thrashes per minute) is represented as a percentage of the wild-type thrashing rate, which is 152.44 ± 6.9 thrashes per minute. Error bars show the standard error of the mean. n = 50 animals. (C) Quantitation of young adult animals exhibiting displaced GABA neurons reveals that late-onset transient *sax-7* expression cannot rescue the *sax-7*-related displaced neurons in the different mutant backgrounds.

levels in *gtl-2* animals (Teramoto *et al.* 2010). Consistent with this finding, the *sax-7 gtl-2* growth rate was recovered by culturing *sax-7 gtl-2* animals on media with reduced Mg^{2+} levels. Reduced Mg^{2+} levels also suppressed the *sax-7 gtl-2* Con, Egl, and lethargic phenotypes as well as the synthetic coiling and Ric phenotypes, supporting the idea that increased systemic Mg^{2+} levels contribute, in large part, to these apparent neuromuscular phenotypes.

Although it was previously shown that systemic ion homeostasis contributes to neuronal network excitation/inhibition balance in *C. elegans* (Stawicki *et al.* 2011), it is not clear how the increased systemic levels of Mg^{2+} may affect neuromuscular function. Similar to *gtl-2* animals, patients suffering from hypermagnesemia also present clinically with neuromuscular symptoms that include lethargy, paralysis-inducing deep tendon reflex loss, and impaired cardiac functions. These symptoms are thought to arise in part from the inhibitory actions of Mg^{2+} on neurotransmission, voltage-gated calcium channels, and the ryanodine receptor (Mordes and Wacker 1977; Lansman *et al.* 1986; Sonna *et al.* 1996; Topf and Murray 2003; Wang *et al.* 2004; Laver 2007; Wang and Berlin 2007; Alexander *et al.* 2008). It is possible that these processes in *C. elegans* are similarly affected by the increased systemic Mg^{2+} levels in *gtl-2* backgrounds. Alternatively and/or additionally, the abnormal Mg^{2+} levels may simply have a negative impact on general animal health that indirectly affects neuromuscular function.

In addition to Mg^{2+}, other divalent ions regulated by *gtl-2* may also contribute to the *sax-7 gtl-2* synthetic phenotypes. TRPM channels are permeable to Ca^{2+} and trace metal ions, including Zn^{2+} and Ni^{2+} (Monteilh-Zoller *et al.* 2003; Georgiev *et al.* 2010; Nilius and Owsianik 2011). Indeed, besides being hypermagnesemic, *gtl-2* mutant animals also have reduced systemic Ca^{2+} levels, which are likely to also influence neuromuscular activity (Teramoto *et al.* 2010). Furthermore, metal ions were implicated in the *gtl-2*-related suppression of convulsions that resulted from *acr-2* hyperactivity (Stawicki *et al.* 2011).

The role of sax-7 in the sax-7 gtl-2 synthetic phenotypes

It is interesting that no overt abnormalities in nervous system function are observed in *sax-7* animals, despite progressive displacement of neurons and their processes. It is only in sensitized *gtl-2*, *unc-13*(*n2813*), and *rab-3* backgrounds where synaptic activity is modestly altered that loss of *sax-7* function can cause synthetic phenotypes that implicate neurotransmission defects. The genetic interaction between *sax-7* and *rab-3* null alleles suggests that *sax-7* functions in a process distinct from that of *rab-3*. In contrast, we are unable to discern whether *sax-7* functions together with *unc-13* or in an *unc-13* parallel pathway. Because UNC-13 is a core component of the neurotransmission machinery, loss of *unc-13* function results in a severe phenotype that cannot be further enhanced. As a result, the genetic interaction with *sax-7* can be observed only with weaker hypomorphic *unc-13* alleles. Importantly, the use of tissue-specific and inducible *sax-7* expression systems to successfully rescue the synthetic phenotypes but not neuronal displacement reveals a novel function for *sax-7* in neurons that is distinct from its well-characterized role in maintaining neural architecture. When taken together, these findings point to this novel *sax-7* role as having apparent modulatory activity on synaptic function.

Previous studies have implicated L1CAMs in synapse formation and maturation. For example, L1 has been shown to act transcellularly to organize nicotinic cholinergic synapses (Triana-Baltzer *et al.* 2006, 2008). Moreover, a previous study revealed a role for the *Drosophila* L1CAM neuroglian in central synapse formation (Godenschwege *et al.* 2006). While it is possible that *sax-7* participates in synapse

formation, we think this is unlikely to contribute to the synthetic phenotypes we observed. First, examination of *sax-7 gtl-2* cholinergic and GABAergic synapses revealed no overt morphological abnormalities. Second, suppression of the synthetic *sax-7 gtl-2* Ric and *unc-13*; *sax-7* movement phenotypes by late-onset transient *sax-7* expression in L4-staged animals, a time when mature synapses have long been formed, strongly argues against a role for *sax-7* in a developmental process such as synaptogenesis. Instead, the temporal nature of this *sax-7* rescuing activity is more in line with *sax-7* having an acute role in nervous system function, such as modulating synaptic activity. It is not clear how *sax-7* may influence synaptic function, but one possibility stems from a previous study demonstrating a role for CHL1 in regulating recycling of synaptic vesicles (Leshchyns'ka *et al.* 2006). A reduced rate of synaptic vesicle recycling could account for the observed synthetic phenotypes in *sax-7* mutant backgrounds.

Supporting this possibility is the significantly reduced thrash rate observed in *sax-7* animals when placed in liquid, despite generally normal locomotion on agar, a solid substrate. In contrast to locomotion on solid agar surfaces, the demand on synaptic function is far greater for animals in liquid to execute the quick and continuous thrashing movements. A reduced synaptic vesicle recycling rate, even at modest levels, is likely to be magnified in such an assay.

Modifier genes in uncovering novel L1CAM functions

Modifier gene studies have been essential in revealing mechanisms underlying cellular processes and signal transduction pathways (St. Johnston 2002). For example, much of our understanding of the MAP kinase signaling pathway as well as *C. elegans* vulval development stemmed from genetic modifier screens that identified suppressors or enhancers of vulval phenotypes (Fay and Yochem 2007; Sundaram 2013). Such modifier gene studies not only reveal mechanisms of cellular processes, but often also uncover novel roles for genes that may be masked by genetic redundancies or other essential functions. Indeed, a previous study uncovered a nonneuronal role for SAX-7 in gastrulation that was made evident only in the absence of HMR-1/cadherin because of functional redundancy by both genes in this process (Grana *et al.* 2010). Mammalian L1CAMs have also been shown to act as modifier genes. For example, *L1* acts as a modifier for intestinal aganglionosis, genetically interacting with the endothelin signaling pathway during enteric nervous system development (Wallace *et al.* 2010, 2011). In addition, *Nrcam* acts as a modifier gene in peripheral neuropathy, genetically interacting with *Lpin1* to synergistically cause progressive hindlimb paralysis. This genetic interaction demonstrates that in addition to the well-characterized neuronal developmental roles, NrCAM is also important for adult nervous system function (Douglas *et al.* 2009). In our study, we demonstrate that *sax-7* has a previously uncharacterized neuronal role that was uncovered only in sensitized backgrounds with abnormal synaptic function. Similar genetic interactions by L1CAMs with synaptic genes in humans may account for some of the heterogeneity of the CRASH symptoms in the L1 disorder as well as complex neuropsychiatric disorders, addiction, and autism associated with L1CAMs.

Acknowledgments

We thank the *C. elegans* community at the University of Minnesota, in particular Jocelyn Shaw, David Greenstein, and Brock Grill for intellectual discussion, as well as the Caenorhaditis Genetics Center and The Japanese National Bioresource Project for providing strains used in this study. This study was made possible by grant NS045873 from the National Institute of Neurological Disorders and Stroke.

Literature Cited

Alexander, R. T., J. G. Hoenderop, and R. J. Bindels, 2008 Molecular determinants of magnesium homeostasis: insights from human disease. J. Am. Soc. Nephrol. 19: 1451–1458.

Alfonso, A., K. Grundahl, J. R. McManus, and J. B. Rand, 1994 Cloning and characterization of the choline acetyltransferase structural gene (cha-1) from C. elegans. J. Neurosci. 14: 2290–2300.

Altun-Gultekin, Z., Y. Andachi, E. L. Tsalik, D. Pilgrim, Y. Kohara *et al.*, 2001 A regulatory cascade of three homeobox genes, ceh-10, ttx-3 and ceh-23, controls cell fate specification of a defined interneuron class in C. elegans. Development 128: 1951–1969.

Anderson, R. B., K. N. Turner, A. G. Nikonenko, J. Hemperly, M. Schachner *et al.*, 2006 The cell adhesion molecule l1 is required for chain migration of neural crest cells in the developing mouse gut. Gastroenterology 130: 1221–1232.

Backer, S., T. Sakurai, M. Grumet, C. Sotelo, and E. Bloch-Gallego, 2002 Nr-CAM and TAG-1 are expressed in distinct populations of developing precerebellar and cerebellar neurons. Neuroscience 113: 743–748.

Brenner, S., 1974 The genetics of *Caenorhabditis elegans*. Genetics 77: 71–94.

Chen, L., and S. Zhou, 2010 "CRASH"ing with the worm: insights into L1CAM functions and mechanisms. Dev. Dyn. 239: 1490–1501.

Chen, L., B. Ong, and V. Bennett, 2001 LAD-1, the Caenorhabditis elegans L1CAM homologue, participates in embryonic and gonadal morphogenesis and is a substrate for fibroblast growth factor receptor pathway-dependent phosphotyrosine-based signaling. J. Cell Biol. 154: 841–855.

Davis, M. W., M. Hammarlund, T. Harrach, P. Hullett, S. Olsen *et al.*, 2005 Rapid single nucleotide polymorphism mapping in C. elegans. BMC Genomics 6: 118.

Dong, X., O. W. Liu, A. S. Howell, and K. Shen, 2013 An extracellular adhesion molecule complex patterns dendritic branching and morphogenesis. Cell 155: 296–307.

Douglas, D. S., J. L. Moran, J. R. Bermingham, Jr., X. J. Chen, D. N. Brindley *et al.*, 2009 Concurrent Lpin1 and Nrcam mouse mutations result in severe peripheral neuropathy with transitory hindlimb paralysis. J. Neurosci. 29: 12089–12100.

Fay, D. S., and J. Yochem, 2007 The SynMuv genes of Caenorhabditis elegans in vulval development and beyond. Dev. Biol. 306: 1–9.

Fernandez, R. M., R. Nunez-Torres, L. Garcia-Diaz, J. C. de Agustin, G. Antinolo *et al.*, 2012 Association of X-linked hydrocephalus and Hirschsprung disease: report of a new patient with a mutation in the L1CAM gene. Am. J. Med. Genet. A 158A: 816–820.

Fleming, J. T., M. D. Squire, T. M. Barnes, C. Tornoe, K. Matsuda *et al.*, 1997 Caenorhabditis elegans levamisole resistance genes lev-1, unc-29, and unc-38 encode functional nicotinic acetylcholine receptor subunits. J. Neurosci. 17: 5843–5857.

Fransen, E., G. Van Camp, R. D'Hooge, L. Vits, and P. J. Willems, 1998 Genotype-phenotype correlation in L1 associated diseases. J. Med. Genet. 35: 399–404.

Georgiev, P., H. Okkenhaug, A. Drews, D. Wright, S. Lambert *et al.*, 2010 TRPM channels mediate zinc homeostasis and cellular growth during Drosophila larval development. Cell Metab. 12: 386–397.

Gilleard, J. S., J. D. Barry, and I. L. Johnstone, 1997 cis regulatory requirements for hypodermal cell-specific expression of the Caenorhabditis elegans cuticle collagen gene dpy-7. Mol. Cell. Biol. 17: 2301–2311.

Godenschwege, T. A., L. V. Kristiansen, S. B. Uthaman, M. Hortsch, and R. K. Murphey, 2006 A conserved role for Drosophila Neuroglian and human L1-CAM in central-synapse formation. Curr. Biol. 16: 12–23.

Gracheva, E. O., G. Hadwiger, M. L. Nonet, and J. E. Richmond, 2008 Direct interactions between C. elegans RAB-3 and Rim provide a mechanism to target vesicles to the presynaptic density. Neurosci. Lett. 444: 137–142.

Grana, T. M., E. A. Cox, A. M. Lynch, and J. Hardin, 2010 SAX-7/L1CAM and HMR-1/cadherin function redundantly in blastomere compaction and non-muscle myosin accumulation during Caenorhabditis elegans gastrulation. Dev. Biol. 344: 731–744.

Hallam, S. J., and Y. Jin, 1998 lin-14 regulates the timing of synaptic remodelling in Caenorhabditis elegans. Nature 395: 78–82.

Harris, T. W., E. Hartwieg, H. R. Horvitz, and E. M. Jorgensen, 2000 Mutations in synaptojanin disrupt synaptic vesicle recycling. J. Cell Biol. 150: 589–600.

Jackson, S. R., Y. S. Guner, R. Woo, L. M. Randolph, H. Ford *et al.*, 2009 L1CAM mutation in association with X-linked hydrocephalus and Hirschsprung's disease. Pediatr. Surg. Int. 25: 823–825.

Jouet, M., A. Moncla, J. Paterson, C. McKeown, A. Fryer *et al.*, 1995 New domains of neural cell-adhesion molecule L1 implicated in X-linked hydrocephalus and MASA syndrome. Am. J. Hum. Genet. 56: 1304–1314.

Kohn, R. E., J. S. Duerr, J. R. McManus, A. Duke, T. L. Rakow *et al.*, 2000 Expression of multiple UNC-13 proteins in the Caenorhabditis elegans nervous system. Mol. Biol. Cell 11: 3441–3452.

Lansman, J. B., P. Hess, and R. W. Tsien, 1986 Blockade of current through single calcium channels by Cd2+, Mg2+, and Ca2+. Voltage and concentration dependence of calcium entry into the pore. J. Gen. Physiol. 88: 321–347.

Laver, D. R., 2007 Ca2+ stores regulate ryanodine receptor Ca2+ release channels via luminal and cytosolic Ca2+ sites. Clin. Exp. Pharmacol. Physiol. 34: 889–896.

Leshchyns'ka, I., V. Sytnyk, M. Richter, A. Andreyeva, D. Puchkov *et al.*, 2006 The adhesion molecule CHL1 regulates uncoating of clathrin-coated synaptic vesicles. Neuron 52: 1011–1025.

Lewis, J. A., C. H. Wu, J. H. Levine, and H. Berg, 1980 Levamisole-resistant mutants of the nematode Caenorhabditis elegans appear to lack pharmacological acetylcholine receptors. Neuroscience 5: 967–989.

Lickteig, K. M., J. S. Duerr, D. L. Frisby, D. H. Hall, J. B. Rand *et al.*, 2001 Regulation of neurotransmitter vesicles by the homeodomain protein UNC-4 and its transcriptional corepressor UNC-37/groucho in Caenorhabditis elegans cholinergic motor neurons. J. Neurosci. 21: 2001–2014.

Liljelund, P., P. Ghosh, and A. N. van den Pol, 1994 Expression of the neural axon adhesion molecule L1 in the developing and adult rat brain. J. Biol. Chem. 269: 32886–32895.

McIntire, S. L., R. J. Reimer, K. Schuske, R. H. Edwards, and E. M. Jorgensen, 1997 Identification and characterization of the vesicular GABA transporter. Nature 389: 870–876.

Mello, C. C., J. M. Kramer, D. Stinchcomb, and V. Ambros, 1991 Efficient gene transfer in C. elegans: extrachromosomal maintenance and integration of transforming sequences. EMBO J. 10: 3959–3970.

Miller, K. G., A. Alfonso, M. Nguyen, J. A. Crowell, C. D. Johnson *et al.*, 1996 A genetic selection for Caenorhabditis elegans synaptic transmission mutants. Proc. Natl. Acad. Sci. USA 93: 12593–12598.

Monteilh-Zoller, M. K., M. C. Hermosura, M. J. Nadler, A. M. Scharenberg, R. Penner *et al.*, 2003 TRPM7 provides an ion channel mechanism for cellular entry of trace metal ions. J. Gen. Physiol. 121: 49–60.

Mordes, J. P., and W. E. Wacker, 1977 Excess magnesium. Pharmacol. Rev. 29: 273–300.

Nguyen, M., A. Alfonso, C. D. Johnson, and J. B. Rand, 1995 *Caenorhabditis elegans* mutants resistant to inhibitors of acetylcholinesterase. Genetics 140: 527–535.

Nikonenko, A. G., M. Sun, E. Lepsveridze, I. Apostolova, I. Petrova *et al.*, 2006 Enhanced perisomatic inhibition and impaired long-term potentiation in the CA1 region of juvenile CHL1-deficient mice. Eur. J. Neurosci. 23: 1839–1852.

Nilius, B., and G. Owsianik, 2011 The transient receptor potential family of ion channels. Genome Biol. 12: 218.

Nonet, M. L., J. E. Staunton, M. P. Kilgard, T. Fergestad, E. Hartwieg *et al.*, 1997 Caenorhabditis elegans rab-3 mutant synapses exhibit impaired function and are partially depleted of vesicles. J. Neurosci. 17: 8061–8073.

Okamoto, N., Y. Wada, and M. Goto, 1997 Hydrocephalus and Hirschsprung's disease in a patient with a mutation of L1CAM. J. Med. Genet. 34: 670–671.

Okkema, P. G., S. W. Harrison, V. Plunger, A. Aryana, and A. Fire, 1993 Sequence requirements for myosin gene expression and regulation in *Caenorhabditis elegans*. Genetics 135: 385–404.

Parisi, M. A., R. P. Kapur, I. Neilson, R. M. Hofstra, L. W. Holloway *et al.*, 2002 Hydrocephalus and intestinal aganglionosis: Is L1CAM a modifier gene in Hirschsprung disease? Am. J. Med. Genet. 108: 51–56.

Rand, J. B., and R. L. Russell, 1984 Choline acetyltransferase-deficient mutants of the nematode *Caenorhabditis elegans*. Genetics 106: 227–248.

Saifee, O., L. Wei, and M. L. Nonet, 1998 The Caenorhabditis elegans unc-64 locus encodes a syntaxin that interacts genetically with synaptobrevin. Mol. Biol. Cell 9: 1235–1252.

Sakurai, T., 2012 The role of NrCAM in neural development and disorders–beyond a simple glue in the brain. Mol. Cell. Neurosci. 49: 351–363.

Salzberg, Y., C. A. Diaz-Balzac, N. J. Ramirez-Suarez, M. Attreed, E. Tecle *et al.*, 2013 Skin-derived cues control arborization of sensory dendrites in Caenorhabditis elegans. Cell 155: 308–320.

Sasakura, H., H. Inada, A. Kuhara, E. Fusaoka, D. Takemoto *et al.*, 2005 Maintenance of neuronal positions in organized ganglia by SAX-7, a Caenorhabditis elegans homologue of L1. EMBO J. 24: 1477–1488.

Schrander-Stumpel, C., C. Howeler, M. Jones, A. Sommer, C. Stevens *et al.*, 1995 Spectrum of X-linked hydrocephalus (HSAS), MASA syndrome, and complicated spastic paraplegia (SPG1): clinical review with six additional families. Am. J. Med. Genet. 57: 107–116.

Sieburth, D., Q. Ch'ng, M. Dybbs, M. Tavazoie, S. Kennedy *et al.*, 2005 Systematic analysis of genes required for synapse structure and function. Nature 436: 510–517.

Sonna, L. A., C. A. Hirshman, and T. L. Croxton, 1996 Role of calcium channel blockade in relaxation of tracheal smooth muscle by extracellular Mg2+. Am. J. Physiol. 271: L251–L257.

St. Johnston, D., 2002 The art and design of genetic screens: Drosophila melanogaster. Nat. Rev. Genet. 3: 176–188.

Stawicki, T. M., K. Zhou, J. Yochem, L. Chen, and Y. Jin, 2011 TRPM channels modulate epileptic-like convulsions via systemic ion homeostasis. Curr. Biol. 21: 883–888.

Sulston, J. E., E. Schierenberg, J. G. White, and J. N. Thomson, 1983 The embryonic cell lineage of the nematode Caenorhabditis elegans. Dev. Biol. 100: 64–119.

Sundaram, M. V., 2013 Canonical RTK-Ras-ERK signaling and related alternative pathways (July 1, 2013), *WormBook*, ed. The *C. elegans* Research Community, WormBook, doi/10.1895/wormbook.1.80.2, http://www.wormbook.org.

Suzuki, N., M. Buechner, K. Nishiwaki, D. H. Hall, H. Nakanishi *et al.*, 2001 A putative GDP-GTP exchange factor is required for development of the excretory cell in Caenorhabditis elegans. EMBO Rep. 2: 530–535.

Takenouchi, T., M. Nakazawa, Y. Kanemura, S. Shimozato, M. Yamasaki *et al.*, 2012 Hydrocephalus with Hirschsprung disease: severe end of X-linked hydrocephalus spectrum. Am. J. Med. Genet. A 158A: 812–815.

Teramoto, T., L. A. Sternick, E. Kage-Nakadai, S. Sajjadi, J. Siembida *et al.*, 2010 Magnesium excretion in C. elegans requires the activity of the GTL-2 TRPM channel. PLoS ONE 5: e9589.

Topf, J. M., and P. T. Murray, 2003 Hypomagnesemia and hypermagnesemia. Rev. Endocr. Metab. Disord. 4: 195–206.

Triana-Baltzer, G. B., Z. Liu, and D. K. Berg, 2006 Pre- and postsynaptic actions of L1-CAM in nicotinic pathways. Mol. Cell. Neurosci. 33: 214–226.

Triana-Baltzer, G. B., Z. Liu, N. V. Gounko, and D. K. Berg, 2008 Multiple cell adhesion molecules shaping a complex nicotinic synapse on neurons. Mol. Cell. Neurosci. 39: 74–82.

Troemel, E. R., J. H. Chou, N. D. Dwyer, H. A. Colbert, and C. I. Bargmann, 1995 Divergent seven transmembrane receptors are candidate chemosensory receptors in C. elegans. Cell 83: 207–218.

Turner, K. N., M. Schachner, and R. B. Anderson, 2009 Cell adhesion molecule L1 affects the rate of differentiation of enteric neurons in the developing gut. Dev. Dyn. 238: 708–715.

Venkatachalam, K., and C. Montell, 2007 TRP channels. Annu. Rev. Biochem. 76: 387–417.

Wallace, A. S., C. Schmidt, M. Schachner, M. Wegner, and R. B. Anderson, 2010 L1cam acts as a modifier gene during enteric nervous system development. Neurobiol. Dis. 40: 622–633.

Wallace, A. S., M. X. Tan, M. Schachner, and R. B. Anderson, 2011 L1cam acts as a modifier gene for members of the endothelin signalling pathway during enteric nervous system development. Neurogastroenterol. Motil. 23: e510–e522.

Wang, B., H. Williams, J. S. Du, J. Terrett, and S. Kenwrick, 1998 Alternative splicing of human NrCAM in neural and non-neural tissues. Mol. Cell. Neurosci. 10: 287–295.

Wang, M., and J. R. Berlin, 2007 Voltage-dependent modulation of L-type calcium currents by intracellular magnesium in rat ventricular myocytes. Arch. Biochem. Biophys. 458: 65–72.

Wang, M., M. Tashiro, and J. R. Berlin, 2004 Regulation of L-type calcium current by intracellular magnesium in rat cardiac myocytes. J. Physiol. 555: 383–396.

Wang, X., J. Kweon, S. Larson, and L. Chen, 2005 A role for the C. elegans L1CAM homologue lad-1/sax-7 in maintaining tissue attachment. Dev. Biol. 284: 273–291.

Yochem, J., T. Gu, and M. Han, 1998 A new marker for mosaic analysis in *Caenorhabditis elegans* indicates a fusion between hyp6 and hyp7, two major components of the hypodermis. Genetics 149: 1323–1334.

Yook, K. J., S. R. Proulx, and E. M. Jorgensen, 2001 Rules of nonallelic noncomplementation at the synapse in *Caenorhabditis elegans*. Genetics 158: 209–220.

Zallen, J. A., S. A. Kirch, and C. I. Bargmann, 1999 Genes required for axon pathfinding and extension in the C. elegans nerve ring. Development 126: 3679–3692.

Zhou, S., and L. Chen, 2011 Neural integrity is maintained by dystrophin in C. elegans. J. Cell Biol. 192: 349–363.

Zhou, S., K. Opperman, X. Wang, and L. Chen, 2008 unc-44 Ankyrin and stn-2 gamma-syntrophin regulate sax-7 L1CAM function in maintaining neuronal positioning in *Caenorhabditis elegans*. Genetics 180: 1429–1443.

Communicating editor: M. V. Sundaram

GENETICS

Supporting Information
http://www.genetics.org/lookup/suppl/doi:10.1534/genetics.114.169581/-/DC1

A Novel Nondevelopmental Role of the SAX-7/L1CAM Cell Adhesion Molecule in Synaptic Regulation in *Caenorhabditis elegans*

Karla Opperman, Melinda Moseley-Alldredge, John Yochem, Leslie Bell, Tony Kanayinkal, and Lihsia Chen

DOI: 10.1534/genetics.114.169581

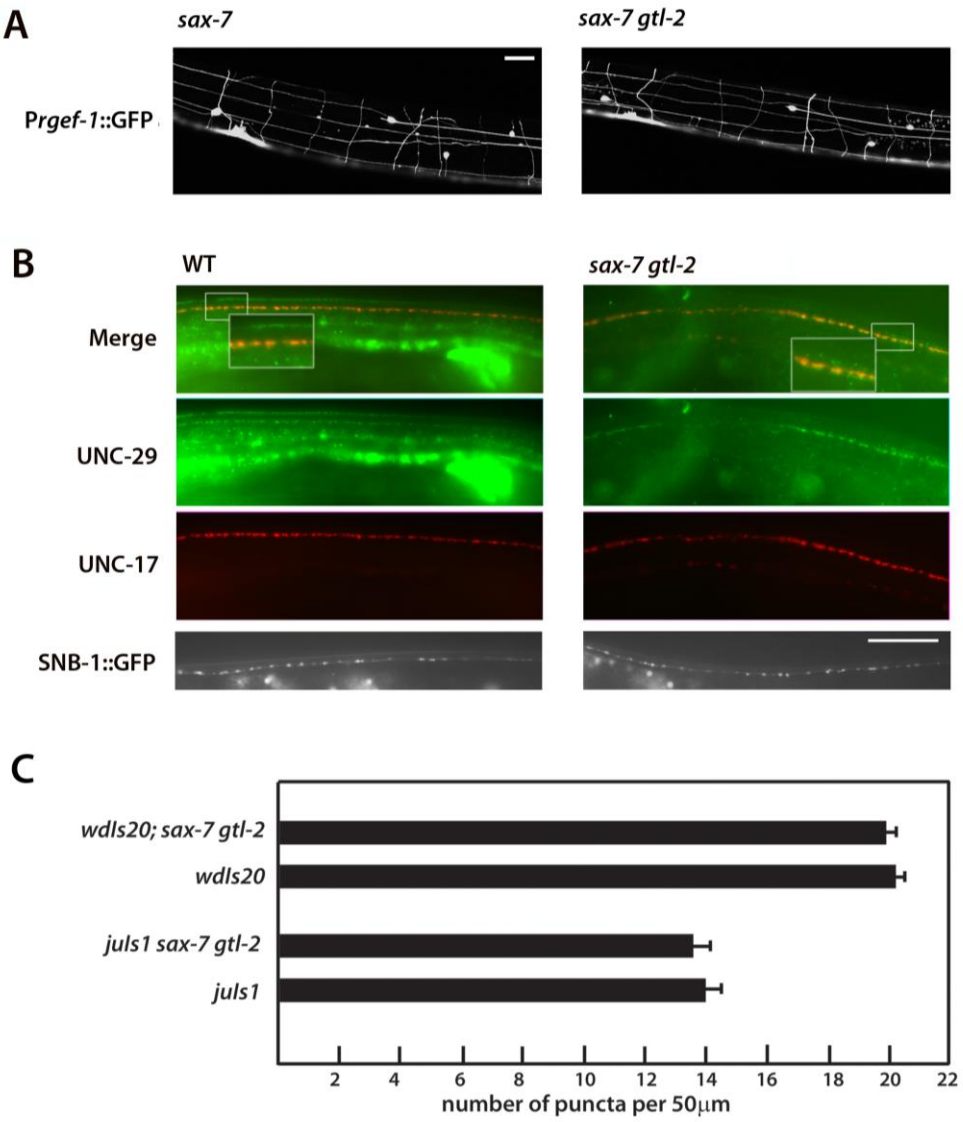

Figure S1 Examination of *sax-7 gtl-2* nervous system and synaptic morphology shows no abnormalities. (A) The *evIs111* (P_{rgef-1}::*gfp*) transgene reveals that the overall nervous system architecture is similar between *sax-7* and *sax-7 gtl-2* animals. (B) Lateral views of the dorsal nerve cord reveal no significant difference in synapses in wild-type and *sax-7 gtl-2* animals, based on antibody staining of cholinergic pre- and post-synaptic proteins, UNC-17 and UNC-29 as well as live imaging of synaptic vesicle protein SNB-1::GFP expressed by the *juIs1* (P_{unc-25}::*snb-1::gfp*) transgene in GABA neurons. Scale bar, 20 μm. (C) Quantitation of SNB-1::GFP puncta over an average distance of 50 μm along wild-type and *sax-7 gtl-2* dorsal nerve cords detected no significant difference in both GABA and cholinergic neurons, as visualized by the *juIs1* and *wdIs20* transgenes, respectively. Error bars show the standard error of the mean. n = 50

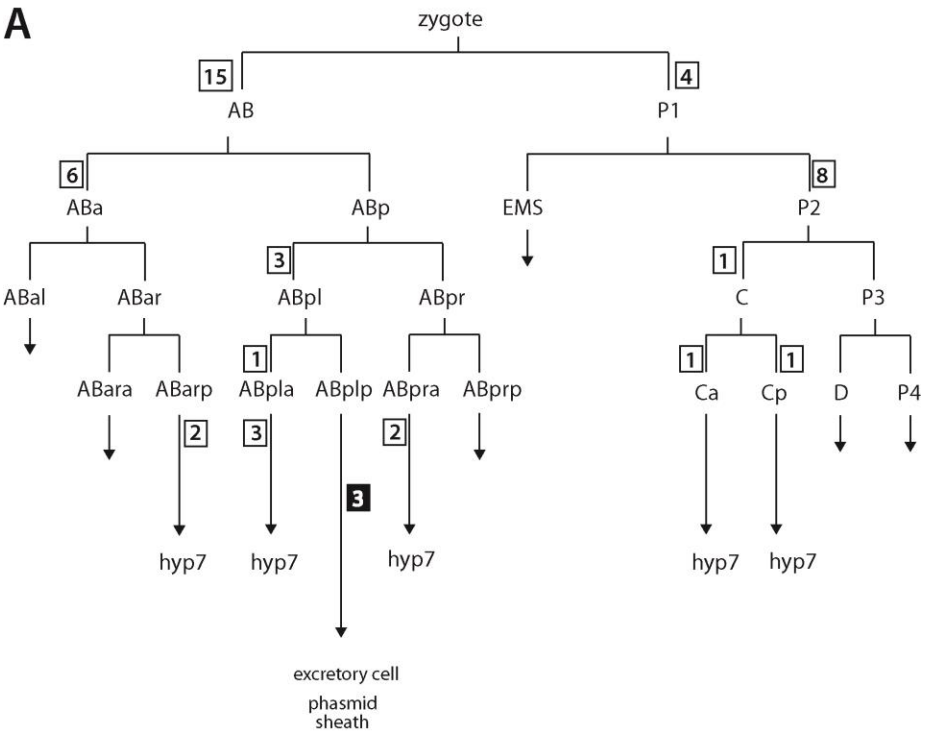

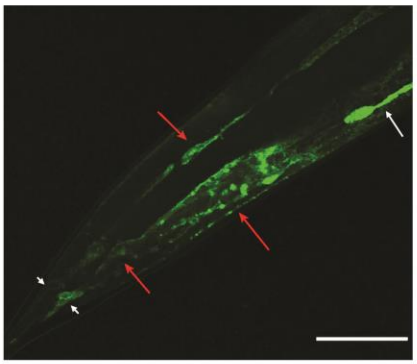

Figure S2 Genetic mosaic analyses implicate hyp7 as a site for action for *gtl-2*. (A) A diagram of the early cell lineage is shown; early embryonic cells that contribute nuclei to the hyp7 syncytium are indicated. The boxed number adjacent to some cells indicates the number of non-mutant mosaic animals that retained the *gtl-2* rescuing transgene in the cell lineage arising from particular cell, but lost the transgene elsewhere due to multiple independent losses of the transgene in other cell lineages. White boxes indicate transgene-positive cell lineage that contribute nuclei to the hyp7 syncytium. The single black box indicates three non-mutant mosaic animals arising from descendents of ABplp, which contribute to two *gtl-2*-expressing tissues, the excretory and phasmid sheath cells, but not to hyp7. Thus, these animals show *gtl-2* expression not in hyp7 but in the excretory cell in two mosaic animals and a phasmid sheath cell in one mosaic animal. As determined by a *gtl-2 ::gfp* construct, *gtl-2* is expressed in (B) hyp7 (red arrows), the excretory cell (long white arrow), and phasmid sheath cells (short arrows). Scale bar, 40 μm